Cellular and Molecular Biology
E-ISSN : 1165-158X / P-ISSN : 0145-5680
www.cellmolbiol.org

Granule Dendrobii suppresses chronic atrophic gastritis induced by N-methyl-N'-nitro-N-nitrosoguanidine by modulating the gastrointestinal bacteria in rats

Caicai Xi [1,2,3,4 #], Kang Feng[2,5 #], Xuan Chen[2,3,4], Hao Wu[1], Hongshan Chen[2], Hui Huang[6], Zeming Ren[2,3,4], Guanhai Dai[2,3,4], Xiaomin Xue[2,3,4], Huifang Zhou[2,7], Zhenmei Lu[1], Renzhao Wu[2,3,4*]

[1] MOE Laboratory of Biosystem Homeostasis and Protection, College of Life Sciences, Zhejiang University, Hangzhou, 310058 P. R. China
[2] Zhejiang Academy of Traditional Chinese Medicine, Hangzhou, 310007 P. R. China
[3] Key Laboratory of Research and Development of Chinese Medicine of Zhejiang Province, Hangzhou, 310007 P. R. China
[4] Key laboratory of pharmacodynamic material basis research in Chinese medicine of Zhejiang province, Hangzhou, 310007 P. R. China
[5] Zhejiang Vocational College of Special Education, Hangzhou, 310023 P. R. China
[6] Institute of Translational Medicine, Zhejiang University, Hangzhou, 310009 P. R. China
[7] School of Basic Medical Sciences, Zhejiang Chinese Medical University, Hangzhou, 310053 P. R.China

#These authors contributed equally to the work and are the co-first authors.

ARTICLE INFO

Original paper

Article history:
Received: May 15, 2023
Accepted: July 22, 2023
Published: July 31, 2023

Keywords:

Chronic atrophic gastritis (CAG), Granule Dendrobii, 16S rRNA sequencing, RT-qPCR

ABSTRACT

Chronic atrophic gastritis (CAG) is an important stage in the transformation of the normal gastric mucosa into gastric cancer. *Granule Dendrobii* (GD), a proprietary Chinese medicine, has proven clinical efficacy in treating CAG. GD might promote the reversal of precancerous lesions by improving them in CAG patients. However, the mechanism of GD in CAG treatment is relatively less understood. Here, N-methyl-N'-nitro-N-nitrosoguanidine (MNNG)-induced CAG rats were treated with GD and its efficacy was evaluated by observing the changes in the rats' weight and the pathology of gastric tissues. The potential effect of GD on the bacteria was predicted and verified in the large and small intestines and stomachs of CAG rats using amplicon sequencing and RT-qPCR. The results showed that GD could ameliorate the symptoms of body weight loss in CAG rats. Hematoxylin-Eosin (HE) and Alcian Blue (AB) staining showed that GD significantly improved the pathological state of the gastric mucosa in CAG rats. The relative abundance (RA) of *Lactobacillus* and *Turicibacter* significantly decreased after GD intervention compared with that of the model group ($P < 0.05$), indicating that GD might improve CAG by regulating the RA of *Lactobacillus* and *Turicibacter*. These findings revealed that *Lactobacillus* and *Turicibacter* as bacteria agents associated with gastritis, have the potential to inhibit gastric cancer, especially *Turicibacter* maybe another pathogen of CAG besides *Helicobacter pylori* (*HP*), which is worthy of further study. Meanwhile, the findings provided new ideas and materials for the research and development of new CAG drugs.

Doi: http://dx.doi.org/10.14715/cmb/2023.69.7.33

Introduction

Chronic atrophic gastritis (CAG) is a complex and refractory gastrointestinal disease that affects people worldwide. During CAG, pathological changes occur in the gastric mucosal layer, causing thinning, disappearance, or thickening of the mucosal base due to atrophy of the gastric mucosal glands. It is often accompanied by inflammation and precancerous lesions, such as intestinal metaplasia (IM) and dysplasia (1-3). The progression from normal tissue to gastric cancer (GC) involves five processes: normal gastric mucosa, CAG, IM, dysplasia, and GC (4). The prevalence of CAG is reported to be approximately 16%, and in countries with a high incidence of GC, it can rise to 27%. The incidence of GC in patients with CAG is 0.004%–0.3% per person annually, indicating that these patients are at a higher risk of GC (5-6). Therefore, improving or even reversing the development process of CAG is not only the goal of CAG treatment but also has great significance for the early identification of neoplasms and reduction in GC mortality.

Traditional Chinese medicine (TCM) has a unique advantage in treating gastrointestinal diseases with reliable therapeutic efficacy and fewer adverse effects. Studies have shown that TCM can reduce or reverse the precancerous lesions of GC, and prevent the development of GC (7-8). *Granule Dendrobii* (GD), a TCM herb composed of *Dendrobium officinale* Kimura et Migo and *Panax quinquefolium* L, is commonly used for treating stomach diseases. Although a previous study showed that GD could effectively treat CAG (9), the underlying mechanism hasn't been explored further. The human gut tract hosts a complex and dynamically changing microbial population referred to as the gut microbiome, which contributes to regulating gastrointestinal function and participates in a variety of physiological and pathological processes that can protect the

* Corresponding author. Email: wufeng03@126.com

human body by aiding in the digestion and synthesis of vitamins. Emerging studies have implicated the dysregulation of the gut microbiome in the pathogenesis of gastrointestinal diseases. Further, changes in the intestinal flora promote the progression of CAG to GC (10-12). Several factors are involved in the pathogenesis of CAG, including *Helicobacter pylori* (*Hp*) infection (13), a major cause of the disease. However, whether there are other pathogenic bacteria remains unknown. With advances in sequencing technology, mainly 16S rRNA sequencing, the pathogenesis of gastrointestinal bacteria (GB) has been gradually revealed (14-15).

Several factors are involved in the pathogenesis of CAG, including Helicobacter pylori (Hp) infection (13), a major cause of the disease. However, N-methyl-N'-nitro-N-nitrosoguanidine (MNNG), a potent mutagen and carcinogen, is often used to establish animal models of CAG (15). In this study, to explore the influence of GD on the GB of CAG model rats induced by MNNG, 16S rRNA amplicon sequencing was used to identify the bacterial community characteristics and search different bacteria flora, and the results were verified using RT-qPCR. This study explained the underlying mechanism of GD intervention in CAG from the perspective of microorganisms. And revealed potential bacterial species which could provide a new insight into the development of novel CAG drugs and reduce the incidence of GC.

Materials and Methods

Chemicals and reagents

GD was purchased from Zhejiang Tianhuang Pharmaceutical Co., Ltd (Zhejiang, China). And the contents of Dendrobium officinale polysaccharide (3 g per bag, contained 0.5g of crude *D. officinale* and 0.4 g of *P. quinquefolium*) (9). MNNG was purchased from Shanghai Lanji Biological Co., Ltd (Shanghai, China). The Trizol reagent was purchased from Bao Bio-engineering Co., Ltd (Dalian, China). The qPCR primers were designed and synthesized by Shanghai Sangong Biological Engineering Co., Ltd (Shanghai, China). All reagents were of analytical grade.

Animals and experimental design

52 six-week-old Wistar-Kyoto (WKY) rats (weighing 160–190 g, half males and half females) were reared at the Center for Animal Experiments of Zhejiang Academy of TCM under alternating light and dark conditions (12 h/12 h). All animal experiments were approved by the Animal Ethics Committee of Tongde Hospital, Zhejiang (Approval Number: (2016)040).

Then, 20 specific pathogen-free WKY rats were randomly selected to be fed a normal diet, while the other rats were randomly selected for modeling, and the rats in the modeling group were given MNNG (167 μg/mL) in their drinking water, which was provided freely for 12 weeks. Then, the gastric tissues were examined by histopathology from the model and normal animals (n = 4/group). After successful modeling, the rats were randomly divided into the model and GD groups (n = 10/group). 10 were randomly selected out of 16 normal rats for the normal group. The normal and model groups were intragastrically administered with 0.9% (w/v) normal saline, while the GD group was intragastrically given 1.2 g/(kg·d) GD. All rats were weighed weekly once. After 8 weeks, the rats were anesthetized, and their gastric tissues were quickly extracted. These tissues were fixed with formalin, embedded with paraffin, sliced into 4-μm thick sections, and stained with hematoxylin and eosin (H&E) and Alcian Blue (AB) for histological examination. Fresh large and small intestine and stomach tissues were cryo-preserved and sent to BGI (SHENZHEN) for Gene sequencing.

Histological evaluation of gastric mucosa

Gastric mucosal inflammation: Semi-quantitative method was used to evaluate the degree of gastric mucosal inflammation. The morphology of the entire gastric mucosa was observed at the microscope low power and 10 visual fields were selected to determine inflammation in the antrum of the gastric tissue. Specifically, referring to the diagnostic criteria of gastritis proposed by Houston in 1994(9), the degree of inflammation was divided into seven grades from 0 to 3 according to the degree of inflammatory cell infiltration. Grade 0: no inflammation; Grade 0.5: the inflammation was observed between 0 to 1 under the microscope; Grade 1: the gastric fovea or the bottom of the inherent gland was infiltrated by multiple chronic inflammatory cells; Grade 1.5: the inflammation was observed between Grade 1 to 2 under a microscope; Grade 2: more inflammatory cells were seen from the fovea of the gastric mucosa to the muscularis mucosa. Grade 2.5: the inflammation was observed between Grade 2 to 3 under a microscope; Grade 3: clusters of inflammatory cells were seen in the gastric mucosa.

Changes in gland thickness and gland number on gastric mucosa: Five fields of gastric antrum mucosa were selected from each gastric tissue section, the thickness of gastric antrum mucosal glands in each field was measured with a micrometer, and then the average value of 5 fields was obtained (μm) in each section. At 100X power, the total number of glands inherent in the gastric antrum between 0.2 to 1.2 mm in the pyloric ring of gastric tissue in each rat were counted and expressed as "units/mm".

Intestinal metaplasia: The AB staining method was used to observe the intestinal metaplasia of gastric mucosa. The clinical standard of human gastric mucosa IM (none, mild, moderate, severe) was modified to the standard of rat IM (none-mild, moderate, severe). None and mild combined into a grade, i.e., normal rats. None-mild: the surface epithelium with IM or no IM or/and glands account for less than 1/3 of the total mucosal area. Generally, there is a very small amount of positive staining in the deep mucosa of the gastric antrum and positive staining in the superficial part of the stomach body; Moderate: in the total mucosal area, epithelium or/and glands on the IM surface account for 1/3 and 2/3; Severe: In the total mucosal area, IM surface epithelium or/and glands account for more than 1/3 of it.

Atypical hyperplasia: In each section, 5 high-magnification visual fields were taken to observe gastric mucosal epithelial cells to determine whether there were changes in nuclear polymorphism and glandular atypical hyperplasia (mild, moderate, and severe grade report was adopted).

DNA extraction and 16S rRNA sequencing

Individual samples from the normal, model and GD groups were pooled respectively for the 16S rRNA sequencing. Microbial DNA was extracted from each sample using the MagPure Stool DNA KF kit B (Magen, China) following the manufacturer's instructions and quantified with a Qubit Fluorometer using the Qubit dsDNA BR Assay kit (Invitrogen, USA). The DNA quality was checked using electrophoresis with a 1% agarose gel. The variable regions V4 of the bacterial 16S rRNA gene was amplified using specific primers (515F: 5'-GTGCCAGCMGCCGCGGTAA-3' and 806R: 5'-GGACTACHVGGGTWTCTAAT-3'). The PCR products were purified using the Agencourt AMPure XP beads and eluted in an elution buffer. After validating the libraries using the Agilent Technologies 2100 bioanalyzer, they were sequenced on an Illumina HiSeq 2500 platform (BGI, Shenzhen, China) following the standard pipeline, which generated 2 × 250 bp paired-end reads (16).

Bioinformatic analysis

The raw data was filtered to eliminate the adapters and low-quality reads to obtain clean reads. Then, the overlapping paired-end reads were merged with tags clustered to the operational taxonomic units (OTU) at 97% sequence similarity. Taxonomic ranks were assigned to the representative OTU sequences using the Ribosomal Database Project Naive Bayesian Classifier v.2.2. Finally, the alpha and beta diversity of different screened species were analyzed based on the OTUs and taxonomic ranks (17).

RNA isolation and RT-qPCR

Total RNA was extracted from the stomach contents following the manufacturer's instructions. The quality and concentration were measured using a spectrophotometer. Reverse transcription-quantitative polymerase chain reaction (RT-qPCR) was performed with Universal using the internal reference gene according to the instructions. The primers used are shown in Table S1. RNA 500 ng was used for the RT-qPCR, which was performed using the StepOnePlus System (ABI). The $2^{-\Delta Ct}$ method was used for relative quantitative analysis.

Statistical analysis

SPSS 28.0 software was used for statistical analysis. Data were shown as mean ± standard deviation (SD). One-way analysis of variance, the Least Significant Difference test (LSD-T), and Dunnett T3 were used for normal distribution data, and the rank-sum test was used for skewness distribution data. $P < 0.05$ represented the statistical significance (18).

Results

Inhibitory effect of GD on weight loss in MNNG-induced CAG model rats

To explore the effect of GD on the body weight of CAG rats, the rats' weights were obtained once a week (Fig. 1A). The body weight of the MNNG-induced CAG rats before treatment (172.00 ± 39.48 g) was significantly lower than that of the normal rats (261.60 ± 51.94 g, $P < 0.01$), indicating that the model rats were in a pathological state. After GD treatment, the body weights of CAG rats recovered significantly from week 4 to week 8 ($P < 0.01$) and the body weight of CAG rats in week 8 (254.90 ± 42.77 g) gradually approached that of the normal rats (294.6 ± 58.10 g). The results showed that GD could remarkably inhibit the body weight loss of MNNG-induced CAG rats.

Improvement of gastric histomorphology in MNNG-induced CAG rats by GD

To visually observe the improvement of GD on the gastric mucosa of the CAG rats, the pathological sections of gastric mucosa from the rats in each group were stained with HE or AB and observed under a microscope at 100× or 200× (Fig. 1B). Compared with the normal group, the gastric mucosa of the model rats was atrophied and thinner, and the number of glandular organs was decreased. A certain number of lymphocytes and granulocytes were observed. The interstitium was infiltrated with many acute and chronic inflammatory cells visible. The glandular epithelium displayed atypical hyperplasia, and the glandular epithelial cells were disordered and varied in size and shape. AB staining showed that the entire mucosa was blue, indicating that IM was serious. The pathological features were characteristic of CAG and significantly alleviated after the GD intervention. The pathological changes were alleviated and atrophy was improved. The epithelial cells were arranged neatly without defects or exfoliation. Glands were regular in shape with similar size and shape. AB staining showed very light blue, suggesting almost no IM.

After GD treatment in CAG rats for 8 weeks, the levels of gastric mucosal inflammation in the GD group (0.50±0.24) were significantly lower than that of the model group (0.85±0.41, $P < 0.05$, Fig. 1C). The number of glands (43.70±5.25 unit/mm) and the thickness of glands (299.52±46.17 unit/mm) were significantly higher than those in the model group (34.20±4.66 unit/mm, 217.01±42.88 unit/mm, $P < 0.01$) (Fig. 1D-E). The degree of IM was significantly lower than that of the model group ($P < 0.05$) (Fig. 1F). Although there was no statistical significance compared with the model group, atypical hyperplasia in the GD group also showed an improvement trend (Fig. 1G). All these results indicated that GD had a significant therapeutic effect on CAG.

GD changed the composition of GB in MNNG-induced CAG rats

To explore the changes in GB composition in CAG mo-

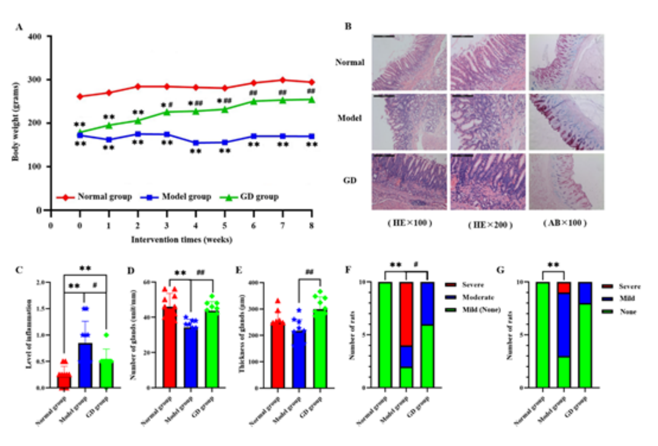

Figure 1. A: Body weight growth curve of each group; B: Histomorphological observation of the rats' gastric mucosa in each group (H&E × 100; H&E × 200; AB × 100); C: The levels of gastric mucosal inflammation in each group rats; D: The number of glands in gastric mucosa in each group rats; E: The thickness of glands in gastric mucosa in each group rats; F: The degree of IM in each group rats; G: The condition of atypical hyperplasia in each group rats. Note: vs. Normal group: * $P < 0.05$, ** $P < 0.01$. vs. Model group: # $P < 0.05$, ## $P < 0.01$.

del rats after intervention with GD, 16S rRNA sequencing was performed using DNA extracted from the large and small intestines and stomachs. The result showed that 25 OTUs decreased after modeling and 58 OTUs increased after GD intervention, in the large intestine. The OTUs decreased by 107 and 41, respectively, after modeling and increased by 36 and 240, respectively, after GD intervention in the small intestine and stomach (Table S2). GD had the greatest impact on the stomach microbiota, indicating that GD might improve CAG by regulating the dynamics of the stomach microbiota.

Based on the Venn diagrams, 828 OTUs were distributed between the three groups, including 611 overlapping OTUs. The normal, model, and GD groups included 720, 714, and 752 OTUs, respectively. Of these, 170 OTUs differed between the model and the normal groups, 126 OTUs differed between the GD and normal groups, and 138 OTUs differed between the GD and the model groups (Fig. 2G). These results showed that the microbiota species changed significantly during the development of CAG lesions and after GD intervention, suggesting that GD might improve CAG by altering the bacterial community.

Alpha and beta diversity were analyzed to determine the changes in the microbial community structure and steady state. The alpha diversity was analyzed to assess the effects of GD on the richness of the GB community in CAG rats. The observed species were selected using Chao, Ace, Shannon, and Simpson indices (Figs. 2A–E). The levels of observed species, Chao, and Ace indices were higher in the GD group than in the model group, which indicated increased richness. The Shannon index levels increased while the Simpson index decreased in the GD group compared with that of the model group, suggesting increased species diversity. The differences in the species complex of the rat groups were analyzed based on the heatmap of the beta diversity evaluated using the Bray–Curtis distance matrix algorithm (Fig. 2F). These results showed that the stomach microbiota was most affected by GD, supporting the OTU analysis results.

GD changed the structures in the GB community in MNNG-induced CAG rats

To further explore the structural changes in the GB community in MNNG-induced CAG rats and the intervention effect of GD, the relative abundance (RA) of the species was compared isolated from the large and small intestines and stomach at the phylum and genus levels (Fig. 3). At the phylum level (Fig. 3A), the GB of each group predominantly consisted of *Firmicutes*, *Bacteroidetes*, *Fusobacteria*, and *Verrucomicrobia*. In the large intestine, the RA of *Bacteroidetes* and *Verrucomicrobia* increased by 9.69% and 7.64%, respectively, after modeling and decreased by 6.66% and 6.02%, respectively, after GD intervention. The RA of *Firmicutes* decreased by 15.09% after modeling and increased by 9.39% after the GD intervention. In the small intestine, the RA of *Fusobacteria* decreased by 9.38% after modeling and increased by 1.66% after GD intervention. In the stomach, the RA of *Bacteroidetes* and *Fusobacteria* decreased by 34.09% and 14.67%, respectively, after modeling and increased by 8.5% and 6.17%, respectively, after GD intervention. The RA of *Firmicutes* increased by 40.61% after modeling and decreased by 24.39% after GD intervention. Therefore, the *Firmicutes* population in the stomach was most affected, which might be closely related to CAG disease.

At the genus level (Fig. 3B), in the large intestine, the RA of *Akkermansia* increased by 7.64% after modeling and decreased by 6.02% after GD intervention. There were similar changes in the RA of *Bacteroides*, *Prevotella*, and *Paraprevotella* in the three rat groups. The RA of *Lactobacillus* increased by 9.39% after modeling and decreased by 9.44% after GD intervention in the small intestine. In the stomach, the RA of *SMB 53* and *Lactobacillus* increased by 30.21% and 4.17%, respectively, after modeling and decreased by 28.35% and 3.9%, respectively, after GD intervention. The RA of *Alcaligenes*, *Mannheimia,* and *Fusobacterium* decreased by 0.08%, 9.95%, and 14.67%, respectively, after modeling and increased by 3.16%, 0.02%, and 6.17%, respectively, after GD intervention. The RA of *Bacteroides* and *Akkermansia* increased by 0.06% and 0.04%, respectively, after the modeling and increased by

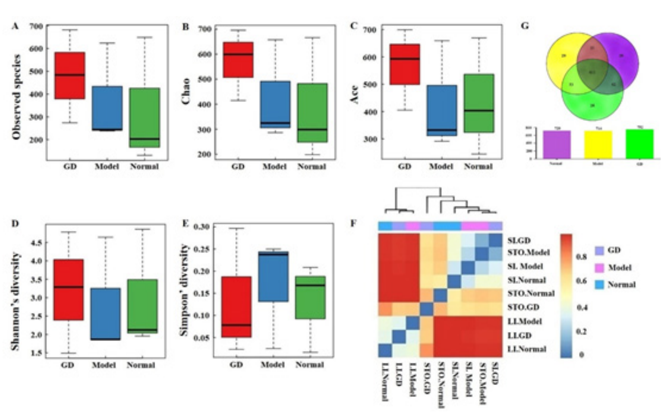

Figure 2. A–E: Alpha diversity within group differences based on Observed species (A), Chao (B), Ace (C), Shannon's diversity (D), Simpson's diversity (E) indices; F: The heatmap of beta diversity distance distribution based on the Bray–Curtis distance matrix algorithm. LI: Large intestine; SI: Small intestine; STO: Stomach. G: Venn diagram displaying the common OTU in GB among the three groups. Different colors represent different groups. The overlapping portions represent the common taxa between the groups, and the nonoverlapping portions represent the unique taxa in each group.

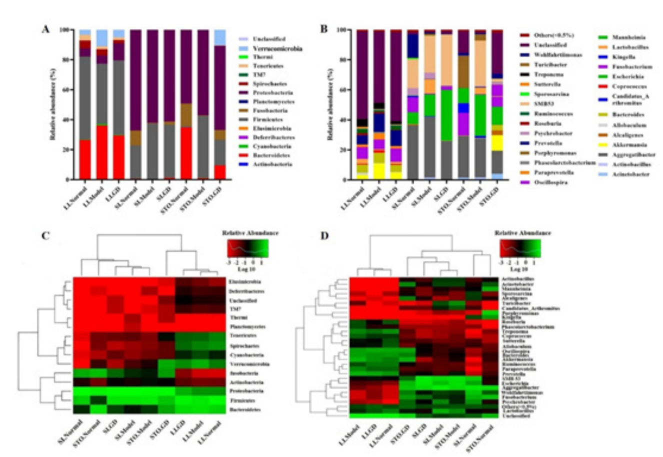

Figure 3. A and B: Histogram of relative abundance during phylum (A) and genus (B). The plotted by the "Relative Abundance" on the Y-axis and "Samples Name" on the X-axis. "Others" represent the total abundance of all other species with an abundance of less than 0.5%; C and D: Heat map based on taxonomy level: phylum (C) and genus (D). Different colors mean the different relative abundance of the taxons in the nine treatments.

3.6% and 10.24%, respectively, after GD intervention. *Turicibacter* appeared after modeling but disappeared after GD intervention. *Porphyromonas* and *Kingella* disappeared after modeling, and no changes were seen after GD intervention.

DEseq2 analysis was used to test the significant differences in microbiota among the normal, model, and GD groups. The results showed that *Turicibacter* was the differentiating species between the model and GD groups ($P < 0.01$). In summary, the RA of *SMB53*, *Akkermansia*, and *Turicibacter* in the stomach was significantly altered after GD intervention, indicating that GD might improve the clinical symptoms of CAG by targeting these GB species, especially *Turicibacter*, which should be further explored.

The differences in the distribution of the dominant bacterial species in each group were analyzed and observed an obvious aggregation effect in the transformation of these groups (Fig. 3C and 3D). After GD treatment, most bacterial phylum from *Bacteroidetes* converted into *Firmicutes* in the large intestine; *Proteobacteria* and *Firmicutes* converted into Fusobacteria and Bacteroidetes in the small intestine, and *Firmicutes* convert into *Verrucomicrobia*, *Fusobacteria, and Bacteroidetes* in the stomach. While *Prevotella*, *Akkermansia*, *Bacteroides*, *Treponema*, *Paraprevotella*, *Roseburia*, *Phascolarctobacterium,* and *Coprococcus* converted into *Oscillospira*, *Ruminococcus,* and *Lactobacillus* in the large intestine, *Aggregatibacter*, *Psychrobacter*, *Acinetobacter*, *Lactobacillus*, *Actinobacillus*, *Turicibacter,* and *Wohlfahrtiimonas* convert into *SMB53*, *Escherichia,* and *Fusobacterium* in the small intestine, *Aggregatibacter*, *Escherichia*, *SMB53*, *Lactobacillus*, *Actinobacillus*, *Candidatus_Arthromitus,* and *Turicibacter* convert into *Akkermansia*, *Oscillospira*, *Fusobacterium*, *Acinetobacter*, *Bacteroides*, *Wohlfahrtiimonas*, *Alcaligenes*, and *Psychrobacter* in the stomach at the genus level. Therefore, the heat map of the dominant bacterial species showed that GD significantly altered the distribution pattern of GB in the large and small intestines and stomachs, suggesting that GD might maintain microbiota homeostasis.

Correlation analysis among superior genera based on network

Gastrointestinal microecological play a crucial role in maintaining human immunity, metabolic homeostasis, and preventing pathogen infection, and niche-specific microbial networks can be reflected the gastrointestinal microenvironment. The correlations among the genus richness were constructed based on the predicted network (Fig. 4). *Lactobacillus*, *Bacteroides*, *Alcaligenes*, *Akkermansia*, *Kingella*, *Mannheimia*, *Porphyromonas* and *SMB53* were highly degreed, indicating that these genera had the strongest actions and could exert potential synergistic effects with GD in treating CAG. However, *Turicibacter* had not be degreed, suggesting it might have little correlation with other genera.

mRNA expression levels of the bacterial genera in the stomach by RT-qPCR

It was found that GD had the highest impact on the stomach flora in the CAG model rats after 16S rRNA amplicon sequencing. Therefore, *Lactobacillus*, *Bacteroides*, *Alcaligenes*, *Akkermansia*, *Kingella*, *Mannheimia*, *Porphyromonas*, *Turicibacter*, *and SMB53* species from the stomach were evaluated using RT-qPCR as their RA was strongly influenced by GD. SPSS was used to analyze whether the differences were significant (Fig. 5). The results indicated that *Lactobacillus*, *Akkermansia*, *Kingella,* and *Turicibacter* showed the same tendency as that of 16S rRNA. SPSS analysis showed statistically significant differences in *Lactobacillus*, *Akkermansia*, *Kingella*, *Mannheimia*, *Porphyromonas,* and *Turicibacter* between the model and the normal groups ($P < 0.01$ or $P < 0.05$), suggesting that these bacterial species might be involved in CAG. Significant differences were observed in *Lactobacillus* and *Turicibacter* between the GD and model groups ($P < 0.05$), indicating that GD might improve CAG by influencing the RA of *Lactobacillus* and *Turicibacter*. Although the changes were observed in other flora, they were not statistically significant. This further verified that GD may alleviate CAG by regulating the dynamics of the stomach flora.

Discussion

As CAG patients are at a higher risk of developing GC,

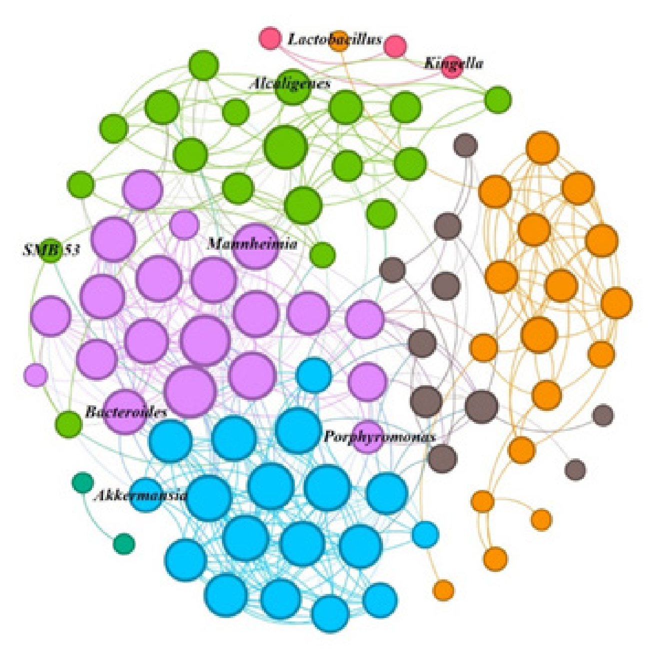

Figure 4. Correlations among genus richness based on network. A connection represents a strong (Spearman's $P > 0.5$) and significant ($P < 0.1$) correlation.

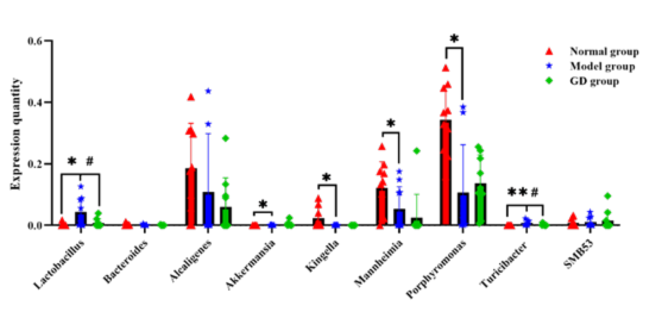

Figure 5. The mRNA expression levels of nine bacterial genera in the stomach. Note: vs. Normal group: * *P < 0.05*, ** *P < 0.01*. vs. Model group: $^{\#}$ *P < 0.05*, $^{\#\#}$ *P < 0.01*.

early detection of tumors and treatment of CAG patients can reduce the mortality due to GC. Therefore, discovering an effective drug for CAG is urgently required. Here, nine bacterial species were found using 16S rRNA data prediction at the genus level and verified using RT-qPCR. The results indicated that *Lactobacillus*, *Akkermansia*, *Kingella*, and *Turicibacter* showed the same tendency as that of 16S rRNA. Among them, the RA of *Lactobacillus* and *Turicibacter* were increased after modeling ($P < 0.01$ or $P < 0.05$) and decreased after GD intervention ($P < 0.05$). This suggests that *Lactobacillus* and *Turicibacter* might be related to GD intervention in CAG.

GD improves CAG by regulating the RA of Lactobacillus.

Lactobacillus is a very common intestinal flora and is a well-known probiotic. It has antibacterial activities, alleviates mucosal inflammation, modulates mucosal immunity, and even has anti-cancer effects on the human stomach. Although a moderate amount of *Lactobacillus* is beneficial to humans, recent reports have shown that the RA of *Lactobacillus* is significantly elevated in GC (19). This phenomenon can be explained using four theories: 1) *Lactobacillus* increases the production of lactic acid and promotes the growth of tumor cells. Furthermore, *Lactobacillus* has been shown to reduce nitrate to nitrite, releasing several N-nitroso compounds that promote mutagenesis, angiogenesis, and protooncogene expression by the epithelial cells, leading to GC (20-21). 2) *Lactobacillus* is an effective inducer of reactive oxygen species in cultured cells and *in vivo*, which can strongly induce DNA damage (22). 3) *Lactobacillus* can enhance the expression of NANOG and transform human fibroblasts into multipotent cells, suggesting that *Lactobacillus* has direct carcinogenic activity (23). 4) *Lactobacillus* itself might not be pathogenic, but it might indirectly promote carcinogenesis by altering the gastric microbial community (24). These theories indicate that *Lactobacillus* is closely related to the occurrence of GC. CAG is an intermediate lesion during GC progression. The significant increase in *Lactobacillus* after CAG modeling is consistent with the gradual rise in the RA of *Lactobacillus* during carcinogenesis (25). This result was consistent with the above study; the RA of *Lactobacillus* increased after modeling and decreased significantly after GD intervention. This suggests that *Lactobacillus* is the key GB species involved in CAG, and GD improves CAG maybe through regulating the RA of *Lactobacillus*.

Turicibacter is a crucial gastrointestinal microbiota in the regulation of CAG by GD

Turicibacter is another important group of the GB that is considered a ‘healthy’ bacterial genus with anti-inflammatory effects (26). However, studies have shown that *Turicibacter* inhibits the proliferation of intestinal flora and its products, causing systemic inflammation. As CAG is a process of inflammatory tumor transformation, continuous inflammatory stimulation promotes the growth of GC cells (26-27). Our results are consistent with previous reports. Unlike the normal group, the modeling group showed the presence of *Turicibacter* and increased inflammation, leading to CAG. This indicates that *Turicibacter* might be another pathogen involved in CAG besides *HP*. However, compared with the model group, CAG improved, and *Turicibacter* disappeared after GD intervention, indicating that GD has anti-inflammatory effects and can inhibit the growth of *Turicibacter*. This further confirmed that *Turicibacter* might be implicated in CAG.

An alternate hypothesis might be that *Turicibacter* might not be pathogenic. As CAG was induced using MNNG, the increase in *Turicibacter* after modeling might be the body’s mechanism to induce more *Turicibacter* in the stomach microbial community to fight inflammation. When the inflammation was reduced, the dynamic balance of the stomach microbial community was readjusted, along with a decrease in the abundance of *Turicibacter*. The above two views suggest that *Turicibacter* is the key GB species targeted by GD during CAG treatment. However, this mechanism needs further research.

Generally, GD can improve the diversity and abundance of GB in CAG rats and hence, improve the clinical symptoms of CAG by modulating GB homeostasis. Among them, *Lactobacillus* and *Turicibacter* are the crucial GB targeted by GD to improve the clinical signs of CAG. *Turicibacter* might be another pathogen of CAG besides *HP*, which should be studied further. In summary, our results provide a theoretical basis for the mechanism underlying GD intervention in CAG. This might facilitate future research and development of novel drugs for CAG to reduce the mortality rate of GC.

Author Contributions

Caicai Xi, Kang Feng, and Hao Wu conceived the project and wrote the manuscript. Xuan Chen performed the main part of the experiments, with contributions from Zeming Ren and Guanhai Dai. Hongshan Chen, Hui Huang, Xiaomin Xue, and Huifang Zhou contributed to the data collection, analysis, and literature review. Zhenmei Lu and Renzhao Wu participated in the project design as well as manuscript draft preparation and revision. All authors read and agreed to the published version of the manuscript.

Acknowledgments

The authors would like to thank Zhejiang Tianhuang Pharmaceutical CO., Ltd for providing the experimental drug, and the technical support of the BGI (SHEN ZHEN) Co., Ltd. for preparing the bacterial 16S rRNA library and Illumina sequencing. Also acknowledged is the Journal of Zhejiang University-SCIENCE Zhejiang University Press for editing the English text of a draft of this manuscript.

Funding

This research was supported financially by Grants 2016ZX09101069 from National Science and Technology Major Project (Major New Drug Development), 81703789 from the National Natural Science Foundation of China, as well as LGF21H270002 and LGF19H280008 from the Natural Science Foundation of Zhejiang Provincial.

Conflicts of Interest

The authors declare no conflict of interest.

References

1. Han LP, Li T Wang, YY Lai, WZ Zhou, HP Niu, ZW Su, J Lv, GY, Zhang GJ, Gao JL, Huang JB Lou ZH Weierning. A Chinese patent medicine, improves chronic atrophic gastritis with intestinal metaplasia. J Ethnopharmacol 2023; 309;226345. DOI: 10.1016/j.jep.2023.116345.

2. Wang B, Zhou W, Zhang H, Wang W, Zhang B, Li S. Exploring the effect of Weifuchun capsule on the toll-like receptor pathway mediated HES6 and immune regulation against chronic atrophic gastritis. J Ethnopharmacol. 2023 Mar 1;303:115930. DOI: 10.1016/j.jep.2022.115930.
3. Zhang ZF, Zhang XG. Chronic atrophic gastritis in different ages in South China: a 10-year retrospective analysis. BMC Gastroenterol 2023; 23: 1-6. DOI: 10.1186/s12876-023-02662-1.
4. Lerch JM, Pai RK, Brown I, Gill AJ, Jain D, Kővári B, Kushima R, Sheahan K, Slavik T, Srivastava A, Lauwers GY, Langner C. Subtyping intestinal metaplasia in patients with chronic atrophic gastritis: an interobserver variability study. Pathology. 2022 Apr;54(3):262-268. doi: 10.1016/j.pathol.2021.12.288.
5. Huang W, Yau Y, Zhu J, Wang Y, Dai Z, Gan H, Qian L, Yang Z. Effect of Electroacupuncture at Zusanli (ST36) on Intestinal Microbiota in Rats With Chronic Atrophic Gastritis. Front Genet. 2022 Feb 23;13:824739. doi: 10.3389/fgene.2022.824739. PMID: 35281809; PMCID: PMC8906781.
6. Yang C, Xiao G, Yixin Z, Benqiong G, Jingbin N, Peng Q, Jianghong L, Guoping L, Yu Z. Study on tongue coating microbes of bitter taste, sticky and greasy taste in chronic atrophic gastritis. J Tradit Chin Med. 2023 Feb;43(1):160-167. doi: 10.19852/j.cnki.jtcm.20221108.004. PMID: 36640008; PMCID: PMC9924668.
7. Huang M, Li S, He Y, Lin C, Sun Y, Li M, Zheng R, Xu R, Lin P, Ke X. Modulation of gastrointestinal bacterial in chronic atrophic gastritis model rats by Chinese and west medicine intervention. Microb Cell Fact. 2021 Feb 2;20(1):31. doi: 10.1186/s12934-021-01525-2. PMID: 33530970; PMCID: PMC7852297.
8. Hao X, Liu Y, Zhou P, Jiang Q, Yang Z, Xu M, Liu S, Zhang S, Wang Y. Integrating Network Pharmacology and Experimental Validation to Investigate the Mechanisms of Huazhuojiedu Decoction to Treat Chronic Atrophic Gastritis. Evid Based Complement Alternat Med. 2020 Dec 7;2020:2638362. doi: 10.1155/2020/2638362. PMID: 33354218; PMCID: PMC7735863.
9. Wu Y, Li Y, Jin XM, Dai GH, Chen X, Tong YL, Ren ZM, Chen Y, Xue XM, Wu RZ. Effects of Granule Dendrobii on chronic atrophic gastritis induced by N-methyl-N'-nitro-N-nitrosoguanidine in rats. World J Gastroenterol. 2022 Aug 28;28(32):4668-4680. doi: 10.3748/wjg.v28.i32.4668. PMID: 36157922; PMCID: PMC9476874.
10. Lu DH, Huang YM, Kong Y, Tao T, Zhu X. Gut microecology: Why our microbes could be key to our health. Biomed pharmacother 2020,;131: 110784. DOI: 10.1016/j.biopha.2020.110784.
11. Chen C, Chen L, Lin L, Jin D, Du Y, Lyu J. Research progress on gut microbiota in patients with gastric cancer, esophageal cancer, and small intestine cancer. Appl Microbiol Biotechnol. 2021 Jun;105(11):4415-4425. doi: 10.1007/s00253-021-11358-z. Epub 2021 May 26. PMID: 34037843.
12. Gomaa EZ. Human gut microbiota/microbiome in health and diseases: a review. Anton Leeuw 2020; 113: 2019-2040. DOI: 10.1007/s10482-020-01474-7.
13. Ye M, Cheng JJ, Jin D. Systematic review and meta-analysis based on the composition of risk factors of chronic atrophic gastritis under gastroscopy detection. Ann Palliat Med 2021; 10; 9742-9751. DOI: 10.21037/apm-21-2063.
14. Zamorano D, Ivulic D, Viver T, Morales F, López-Kostner F, Vidal RM. Microbiota Phenotype Promotes Anastomotic Leakage in a Model of Rats with Ischemic Colon Resection. Microorganisms. 2023 Mar 7;11(3):680. doi: 10.3390/microorganisms11030680.
15. Tong Y, Wang R, Liu X, Tian M, Wang Y, Cui Y, Zou W, Zhao Y. Zuojin Pill ameliorates chronic atrophic gastritis induced by MNNG through TGF-β1/PI3K/Akt axis. J Ethnopharmacol. 2021 May 10;271:113893. doi: 10.1016/j.jep.2021.113893. Epub 2021 Jan 29. PMID: 33524511.
16. Pérez-Losada M, Castro-Nallar E, Laerte Boechat J, Delgado L, Azenha Rama T, Berrios-Farías V, Oliveira M. Nasal Bacteriomes of Patients with Asthma and Allergic Rhinitis Show Unique Composition, Structure, Function and Interactions. Microorganisms. 2023 Mar 7;11(3):683. doi: 10.3390/microorganisms11030683. PMID: 36985258; PMCID: PMC10056468.
17. Zhang N, Li C, Guo Y, Wu HC. Study on the Intervention Effect of Qi Gong Wan Prescription on Patients with Phlegm-Dampness Syndrome of Polycystic Ovary Syndrome Based on Intestinal Flora. Evid Based Complement Alternat Med. 2020 Sep 29;2020:6389034. doi: 10.1155/2020/6389034. PMID: 33062017; PMCID: PMC7545460.
18. Zhang ZX, Li WZ, Jiang DM, Gu L, Li B, Sang CP, Rao DY, Tang ZX, Liu C. Silencing of long non-coding RNA linc01106 suppresses non-small cell lung cancer proliferation, migration and invasion by regulating microRNA-765. All Life 2022; 15: 458-469. DOI: 10.1080/26895293.2022.2059578.
19. Li ZP, Liu JX, Lu LL, Wang LL, Xu L, Guo ZH, Dong QJ. Overgrowth of Lactobacillus in gastric cancer. World J Gastrointest Oncol 2021; 13: 1099-1108. DOI: 10.4251/wjgo.v13.i9.1099.
20. Forsythe SJ, Cole JA. Nitrite accumulation during anaerobic nitrate reduction by binary suspensions of bacteria isolated from the achlorhydric stomach. J Gen Microbiol 1987; 133: 1845-1849. DOI: 10.1099/00221287-133-7-1845.
21. Calmels S, Béréziat JC, Ohshima H, Bartsch H. Bacterial formation of N-nitroso compounds from administered precursors in the rat stomach after omeprazole-induced achlorhydria. Carcinogenesis 1991; 12: 435-439. DOI: 10.1093/carcin/12.3.435.
22. Jones RM, Mercante JW, Neish AS. Reactive oxygen production induced by the gut microbiota: pharmacotherapeutic implications. Curr Med Chem 2012; 19: 1519-1529. DOI: 10.2174/092986712799828283.
23. Ohta K, Kawano R, Ito N. Lactic acid bacteria convert human fibroblasts to multipotent cells. PLoS One 2012; 7: e51866. DOI: 10.1371/journal.pone.0051866.
24. Wang LL, Yu XJ, Zhan SH, Jia SJ, Tian ZB, Dong QJ. Participation of microbiota in the development of gastric cancer. World J Gastroenterol. 2014 May 7;20(17):4948-52. doi: 10.3748/wjg.v20.i17.4948. PMID: 24803806; PMCID: PMC4009526.
25. Wang Z, Gao X, Zeng R, Wu Q, Sun H, Wu W, Zhang X, Sun G, Yan B, Wu L, Ren R, Guo M, Peng L, Yang Y. Changes of the Gastric Mucosal Microbiome Associated With Histological Stages of Gastric Carcinogenesis. Front Microbiol. 2020 May 29;11:997. doi: 10.3389/fmicb.2020.00997. PMID: 32547510; PMCID: PMC7272699.
26. Zhou P, Yang T, Xu M, Zhao Y, Shen P, Wang Y. 16S rRNA sequencing-based evaluation of the protective effects of Hua-Zhuo-Jie-Du on rats with chronic atrophic gastritis. BMC Complement Med Ther. 2022 Mar 16;22(1):71. doi: 10.1186/s12906-022-03542-z. PMID: 35296316; PMCID: PMC8928654.
27. Zhen Z, Xia L, You H, Jingwei Z, Shasha Y, Xinyi W, Wenjing L, Xin Z, Chaomei F. An Integrated Gut Microbiota and Network Pharmacology Study on Fuzi-Lizhong Pill for Treating Diarrhea-Predominant Irritable Bowel Syndrome. Front Pharmacol. 2021 Nov 30;12:746923. doi: 10.3389/fphar.2021.746923. PMID: 34916934; PMCID: PMC8670173.